

## A New Dynamic Simulation of the Main Marmara Fault Earthquake through Incorporation of Stress Perturbation due to 1912 Ganos and 1999 İzmit Earthquakes and Interseismic Stress Load

Yasemin KORKUSUZ ÖZTÜRK <sup>1</sup>, Nurcan MERAL ÖZEL <sup>2</sup>, Ali Özgün KONCA <sup>2</sup>, Şevket ÖZDEN <sup>3</sup>, and Semih ERGİNTAV <sup>4</sup>

- <sup>1</sup> Erzincan Binali Yıldırım University, Earthquake Technologies Institute, Earth Sciences Engineering, Erzincan, Türkiye
- <sup>2</sup> Boğaziçi University, Kandilli Observatory and Earthquake Research Institute, Geophysics, İstanbul, Türkiye
- <sup>3</sup> Erzincan Binali Yıldırım University, Earthquake Technologies Institute, Earthquake Engineering, Erzincan, Türkiye
- <sup>4</sup> Boğaziçi University, Kandilli Observatory and Earthquake Research Institute, Geodesy, İstanbul, Türkiye





## ··· ·•····· INTRODUCTION AND MAIN RESULTS

The Main Marmara Fault poses a high risk due to a ~120 km seismic gap between the 1912 and 1999 Mw7.4 earthquakes. We model a new 3D dynamic rupture scenario that incorporates stress from past events, strain accumulation, coupling, slip rates, historical constraints, and stress perturbation from the 1912 Ganos and 1999 İzmit earthquakes. Results indicate likely rupture of the Avcılar and Princes' Islands segments, with ≤Mw7.4 magnitude and high PGV on İstanbul's European coast.

\*

## Introduction

The North Anatolian Fault Zone (NAFZ) accommodates westward motion of the Anatolian block (20–25 mm/yr) relative to Eurasia. Its western termination, the Main Marmara Fault (MMF), lies in a complex transition between strike-slip and extensional regimes. The MMF poses a critical hazard due to a ~120 km seismic gap left by the 1912 Ganos and 1999 İzmit Mw7.4 earthquakes.

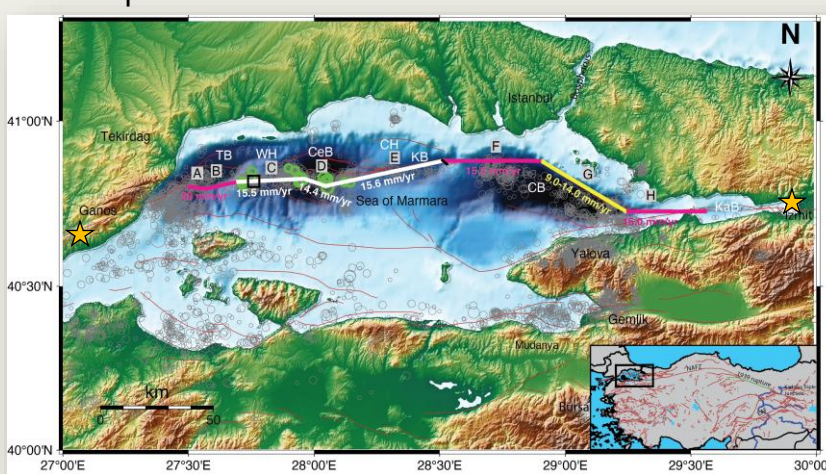


Figure 1. The faults are colored based on the chosen locking depth estimates for the dynamic rupture simulation (Öztürk, et al., 2025), where yellow, white and pink lines indicate 10, 12 and 13 km of locking depth, respectively. Annual slip velocities are also indicated.

We present a new 3D dynamic rupture simulation that incorporates stress perturbations from the 1912 and 1999 events, and we discuss the potential effects of the 23 April 2025 earthquake, which occurred during the process of this study (Öztürk et al., 2025).

## **Methodology for the Quasi-Static Simulation**

- Blocks move beneath the faults (bottom effect), applying stress loading from below.
- Neighboring sliding faults, which ruptured during the 1912 and 1999 earthquakes, drive strain accumulation (side effect) on the unruptured faults.

A uniform 500m hexagonal mesh is used, with the upper crust, lower crust, and mantle assumed to have thicknesses of 20 km, 15 km, and 15 km, respectively.

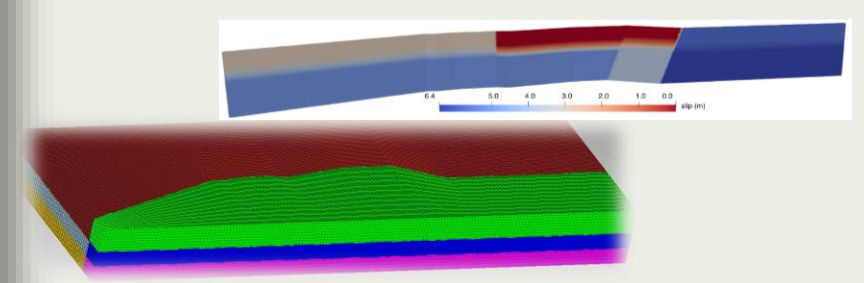


Figure 2. 3D Block model with 3 layers. 2000 m grid size is used for exageration. The initial slip model for the fault surface is shown at the right top for the quasi-static simulation (Red: zero slip).

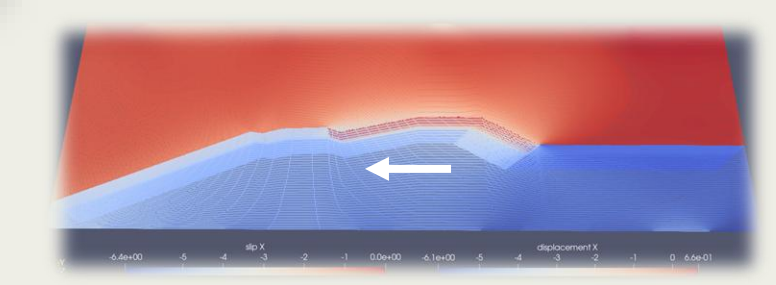


Figure 3. Initial displacement model for the quasi-static simulation .

## Methodology for the Dynamic Simulation

## 1. Compilation of Historical Earthquake Catalog and Determination of Their Rupture Extents

Well-documented damages from historical records and paleoseismological data, especially seismoturbidites obtained from coring from the basins, are compiled.

# 2. Estimation of Initial Along-Strike Shear Tractions The interseismic behavior is analyzed through the annual accumulated slip deficit rate and fault coupling. In addition to this long-term stress accumulation, stress changes calculated during quasi-static simulations are interpolated along the fault.

### 3. Estimation of Normal Tractions

Based on the slip deficit rate, fault coupling, and the elapsed time since the last major earthquake, segment F (Fig. 1) is estimated to be close to failure. According to the Coulomb Failure Criterion, the normal traction on F is calculated by dividing the shear traction by the static friction coefficient. The orientation and magnitude of the maximum principal compressive stress axis  $(\sigma 1)$  are then determined and projected onto the remaining faults.

A logarithmically increasing 200m tetragonal mesh is employed.

Cubit and PyLith (FEM) softwares are used for the generation of geometry and simulations (quasi-static and dynamic), respectively.





## The Fault Geometry and Friction Law

The fault model consists of 8 segments (Armijo et al., 2002) and vertical, with a pure strike-slip behavior except for the PI segment (has a 70° dipping angle).

Dynamic earthquake rupture simulations are generated using a linear slip weakening fault constitutive friction model (Andrews, 1976).

The critical slip distance (Dc) is selected as 0.4 m. Static friction coefficient ( $\mu$ s) and dynamic friction coefficient ( $\mu$ d) are selected as 0.6 and 0.5714, respectively.

The crustal model is homogeneous (Karabulut et al., 2011), where Vp = 6.1 km/s and Vs = 3.5 km/s. Density is 2670.0 kg/ $m^3$  and rigidity is 32 GPa.



Figure 4. Initial (along strike) shear traction distribution on the fault surface for the scenario C1-1.

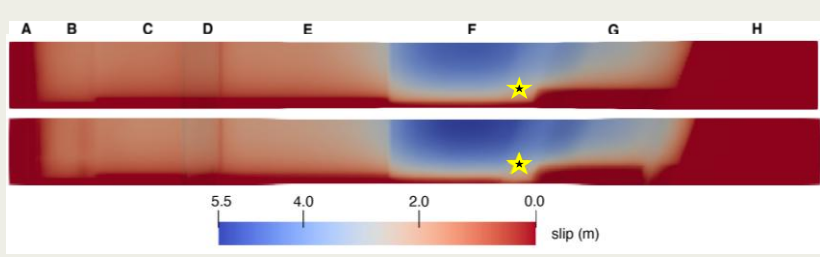
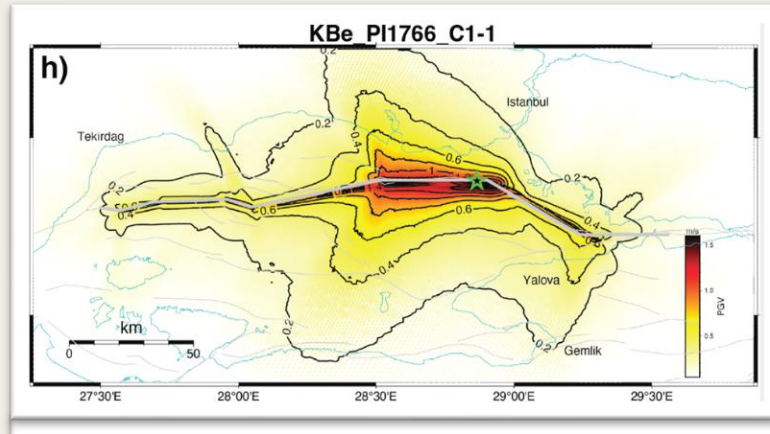


Figure 5. The maximum slip distribution in the along strike direction when stress perturbations due to 1912 and 1999 earthquakes loosed (top) and added (bottom).

## **Results and Discussion**



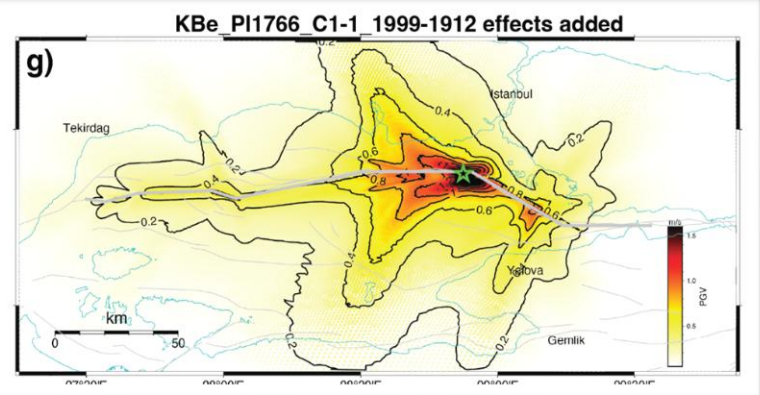


Figure 6. PGV maps for homogeneous half space simulations. Stress change due to 1912 Ganos and 1999 İzmit earthquakes is loosed in (h) and added in (g).

The initial stress distribution is a critical factor for the rupture progression.

The rupture can penetrate the Western Marmara segments under any scenario. The low pre-stress west of the Central Basin does not create a sufficient stress shadow to prevent rupture propagation into the Western Marmara, although the Yalova-Karamürsel segment had been hypothesized to act as a stress shadow zone (due to the 1894 earthquake) that could stop the 1999 İzmit rupture (Harris et al., 2002).

The stress perturbation, calculated via quasi-static simulations, ranges from 0.1 MPa within the segments to 5.0 MPa at their boundaries.

Results from the new dynamic rupture simulation indicate an increase of approximately 40–50 cm in maximum slip -corresponding to an increase of about 0.1 units in moment magnitude- in the central and eastern parts of the MMF (Fig. 5).

Furthermore, higher PGV (Peak Ground Velocity) contours extend into both the European and Asian sides of İstanbul when stress changes from the 1912 and 1999 events are included (Fig. 6).

Faults F and G are assumed to be fully locked, and the aftershock activity of the M6.2 (2025) event reaches their western boundary, implying a high potential for generating a destructive earthquake.



Figure 7. The Main Marmara Fault is shown in black and red lines. Green circles mark repeating earthquakes. The purple star and circles indicate the mainshock and aftershocks of the 23 April 2025 M6.2 earthquake, while the yellow star and circles represent the mainshock and aftershocks of the 26 September 2019 M5.8 earthquake.

## Conclusion

The results are valid if the Ganos (Mürefte) Fault, located at the western boundary of the MMF and unruptured since 1912, is not dynamically triggered.

If all faults rupture together, and assuming the PI segment last ruptured in 1766, the potential MMF event could reach Mw 7.4. In addition, considering that the fault segment affected by the Mw 6.2 event has already ruptured and is largely decoupled, the potential future earthquake could either rupture both Faults F and G together, resulting in an event of Mw ~7.0–7.2, or fault F could rupture independently, generating an earthquake slightly below Mw 7.0, with the Princes' Islands Fault possibly rupturing afterward with a magnitude between Mw 6.2 and 6.8.

Furthermore, higher PGV values are derived in the southern part of the European side of İstanbul and the Marmara Ereğlisi region. The maximum PGV is ~1.5 m/s at the epicenter, decreasing to ~0.6 m/s and 0.8 m/s (when the effects of the 1912 and 1999 earthquakes are included), extending toward the southern part of İstanbul.

The 23 April 2025 Mw 6.2 earthquake likely released the accumulated strain within its rupture area, assuming the validity of our 25% coupling model for faults D and E. This indicates that the fault segment was approximately 25% coupled prior to the event (Öztürk et al., 2025).

## References

Andrews, D. J. (1976). Rupture Velocity of Plane - Strain Shear Cracks. Journal of Geophysical Research, 81, 5679-5687.

Armijo, R., Meyer, B., Navarro, S., King, G., & Barka, A. (2002). Asymmetric slip partitioning in the Sea of Marmara pull-apart: A clue to propagation processes of the north Anatolian Fault? Terra Nova, 14 (2), 80–86.

Harris, R.A., Dolan, J.F., Hartleb, R., & Day, S. M. (2002). The 1999 İzmit, Turkey, Earthquake: A 3D Dynamic Stress Transfer Model of Intraearthquake Triggering. Bulletin of the Seismological Society of America, 92, 1, pp. 245–255.

Karabulut, H., Schmittbuhl, J., Özalaybey, S., Lengliné, O., Kömeç-Mutlu, A., Durand, V., Bouchon, M., Daniel, G., & Bouin, M. P. (2011). Evolution of The Seismicity in the Eastern Marmara Sea a Decade Before and After the 17 August 1999 Izmit Earthquake. Tectonophysics, 510, 17–27.

Öztürk, Y. K., Konca, A. Ö., & Özel, N. M. (2025). 3D dynamic rupture simulations for the potential main Marmara fault earthquake in the sea of Marmara based on the inter-seismic strain accumulation. Journal of Geophysical Research: Solid Earth, 130, e2024JB029585. https://doi.org/10.1029/2024JB029585